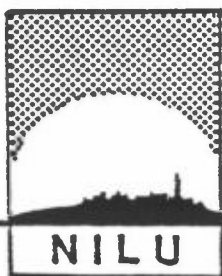


NILU
OPPDRAGSRAPPORT NR 38/80
REFERENCE: 22480
DATE: NOVEMBER 1980

ESTIMATION OF TIMESERIE
MODELS FOR HORIZONTAL WIND.
NORWEGIAN WEST COAST.

BY
KARL J. EIDSVIK



NORWEGIAN INSTITUTE FOR AIR RESEARCH

ROYAL NORWEGIAN COUNCIL FOR SCIENTIFIC AND INDUSTRIAL RESEARCH

NILU
OPPDRAGSRAPPORT NR 38/80
REFERENCE: 22480
DATE: NOVEMBER 1980

ESTIMATION OF TIMESERIE
MODELS FOR HORIZONTAL WIND.
NORWEGIAN WEST COAST.

BY
KARL J. EIDSVIK

NORWEGIAN INSTITUTE FOR AIR RESEARCH
P.O.BOX 130, N-2001 LILLESTRØM
NORWAY

PREFACE

This report is the result of project for IFE in a preliminary effort to utilize NILUs data estimating wind characteristics of relevance to wind energy systems. Making the 5 min. data available demanded most of the resources so there was only a month's work available for data analysis and reporting.

SUMMARY

Timeseries of horizontal wind sampled at intervals of $\Delta t = 5$ min. are analyzed. Power spectra are estimated by fitting an autoregressive model to the data; Akaike's identification procedure is used.

As usual, the low frequency energy dominates in the power spectrum, particularly at the Norwegian west coast stations during the winter season. The typical 5 minute prediction error for wind is estimated to 1 ms^{-1} , and it appears to vary less with the season than the spectral intensity at the lower frequencies.

LIST OF CONTENTS

	Page
PREFACE	2
SUMMARY	2
1 INTRODUCTION	4
2 TIMESERIES MODEL FOR HORIZONTAL WIND	5
2.1 Data	7
3 RESULTS	8
3.1 Broadbanded spectra	8
3.2 West coast spectra	9
3.3 Prediction error	9
4 REMARKS	10
ACKNOWLEDGEMENTS	11
5 REFERENCES	19
APPENDIX A	21
APPENDIX B	22

ESTIMATION OF TIMESERIE MODELS FOR
HORIZONTAL WIND. NORWEGIAN WEST COAST.

1 INTRODUCTION

The main purpose of this study is to estimate a few characteristics of stochastic wind variations that are relevant for wind energy systems. Although such systems may be nonlinear and characterized by absorption or saturation near both ends of the state space, it is for illustrative purposes, assumed that they are described by a set of linear relations

$$L\{\underline{x}(t)\} = \underline{u}(t). \quad (1)$$

Here L is a linear operator and $\underline{x}(t)$ is the time varying n -dimensional state vector. One component could be the instantaneous energy production. \underline{u} is the m -dimensional forcing function (atmospheric variables). Even definitely nonlinear systems may be reasonably well described by Equation (1) when considering deviations from some reference state instead of absolute values (Athans, 1). The solution to Equation (1) over an infinite domain may be written, in component form, as

$$x_i(t) = \int \Gamma_{ij}(\tau) u_j(t-\tau) d\tau. \quad (2)$$

Here Γ is a known transfer function and the summation convention on repeated indicies is used. Equation (2) illustrates that the stochastic properties of the state vector $\underline{x}(t)$ is (in principle) given when the stochastic properties of the forcing function $\underline{u}(t)$ is known.

Or: It illustrates how to design the system (choosing Γ) so that $\underline{x}(t)$ attains favourable stochastic properties when the stochastic properties of $\underline{u}(t)$ are given. Since $\underline{u}(t)$ is a timeserie, \underline{u} (and \underline{x}) have infinitely many stochastic aspects. In this study we will restrict the attention to second order characteristics. From Equation (2) it is easily deduced that the relation between the power spectrum tensors for \underline{x} and \underline{u} and the system transfer function is formally simple

$$\phi_{ij}^x(f) = \{\Gamma_{il}^F(f) \Gamma_{jm}^{F*}(f)\} \phi_{lm}^u(f). \quad (3)$$

Here $\Gamma_{ij}^F(f)$ is the Fourier transform of $\Gamma_{ij}(t)$:

$$\Gamma_{ij}^F(f) = \int \Gamma_{ij}(t) e^{-i2\pi ft} dt \quad (4)$$

O₁: Estimation of $\phi_{lm}^u(f)$ for horizontal wind is one objective for this study.

For optimal control of the system (to extract maximum energy, or avoid wear), it may be necessary to predict \underline{u} over a sufficiently long lead time. For wind energy systems, the control variables may be pitch angle of blades and alignment of the system into the wind.

O₂: Estimation of optimal prediction methods and lower limits to prediction accuracy for horizontal wind over lead times of minutes is another objective for this study.

2 TIMESERIE MODEL FOR HORIZONTAL WIND

Both objectives can be considered as variations over the same theme, namely timeserie modelling (Parzen, 2). Assuming that the $\underline{u}(t)$ -vector is an autoregressive (AR-) process of order p

$$\sum_{i=0}^P \underline{A}(i) \underline{u}(t-i) = \underline{\varepsilon}(t) \quad , \quad (5)$$

the best one-time step ahead prediction is

$$\hat{\underline{u}}(t) = - \sum_{i=1}^P \underline{A}(i) \underline{u}(t-i) \quad . \quad (6)$$

$\underline{A}(i)$ are $p+1$ $m \times m$ dimensional matrices with $\underline{A}(0) = \underline{I}$ and $\underline{\varepsilon}$ is m -dimensional white noise. The prediction error, or innovation variance, is $\underline{V} = E \underline{\varepsilon}(t) \underline{\varepsilon}^T(t)$. Obtaining a co-variance relation by squaring Equation (5), introducing Fourier transforms and utilizing the whiteness of $\varepsilon(t)$, we get as shown in Appendix A:

$$\underline{V}_{ij} = \{ \underline{A}_{in}^F(f) \underline{A}_{jm}^{F*}(f) \} \phi_{nm}^u(f) \quad , \quad (7)$$

with Fourier transform pairs $\underline{A}(k)$, $\underline{A}^F(f)$

$$\underline{A}_{ij}^F(f) = \sum_{k=0}^P \underline{A}_{ij}(k) e^{i2\pi f k} \quad (8)$$

Equation (7) shows how ϕ^u is filtered to produce \underline{V}_{ij} . Since $\underline{A}_{ij}(0) = \delta_{ij}$ and $\underline{A}_{ij}(k)$ is often a negative, rapidly increasing function of $k > 0$, $\{ \underline{A}_{in}^F(f) \underline{A}_{jm}^{F*}(f) \}$ will often be a high pass filter. Equation (7) may also be written

$$\underline{\phi}(f) = \underline{A}^{F^{-1}}(f) \underline{V} \{ \underline{A}^{F^{-1}}(f) \}^* \quad . \quad (9)$$

The spectrum, $\underline{\phi}(f)$, is defined so that its integral between the Nyquist frequencies, $f_N = \pm \frac{1}{2\Delta t}$, is equal to the (co)-variance

$$\underline{E} \underline{u} \underline{u}^T = \int_{-f_N}^{f_N} \underline{\phi}(f) dt \quad (10)$$

Estimating the model as characterized by p , $\underline{A}(i)$ and \underline{V} does therefore also give the spectrum matrix. Akaike's (3) procedure is used for model identification.

Kromer (4), (Gersh and Sharp, 5), has demonstrated that, asymptotically, the spectral density $\underline{\phi}(t)$, computed from a finite AR-model has the statistical properties:

$$E\hat{\phi}(f) \approx \phi(f); \quad \text{var}\hat{\phi}(f) \approx \frac{2P}{N}\phi^2(f) \quad (11)$$

Since the integral scale for atmospheric timeseries may be very large, the limit $N \rightarrow \infty$ may be practically unattainable. The expressions (11) is therefore not taken literary.

2.1 Data

The data were obtained by NILU's automatic weather station. It records the mean wind force over $\Delta t = 5$ minutes and an instantaneous wind direction on the same time resolution. The measurement stations of most interest for wind energy studies were:

Vindenes: (Sotra, Hordaland). Located on a small hill 25 m above the sea surface. Mast: 36 m. Freely exposed to wind from all directions. (Sivertsen 6, 7).

Kårstø: (Karmøy, Rogaland). Located near the sea shore at the bottom of Austreviki, ca 5 m above the sea surface. Mast: 36 m. (Sivertsen, 8).

Årvikafjell: Located on a 226 m hill, ca 2.5 km northeast of Kårstø. Mast: 25 m. (Sivertsen, 8).

Ytraland: (Karmøy, Rogaland). Located 16 m above the sea, ca 500 m from the coastline (North Sea). Mast: 36 m. Surface inhomogenities of typical height scale 10 m.

Dyrholtet: (Mongstad, Hordaland). Located ca 35 m above the sea surface. Mast: 10 m. Shadowed from the dominating wind direction for the area. (Dovland, 9).

Ås: (Herøya, Telemark). Included to illustrate differences between Norwegian west coast and eastern Norway. (Sivertsen and Friberg, 10). Maps are shown in Appendix B. A more detailed description of the station localities and data are found in the referred reports.

A priori and subjectively, it would be natural to consider localities as Ytraland, Vindenes, Årvikafjell and Kårstø as suitable for wind energy sites. The wind statistics at Ytraland and Vindenes are expected to be representative for most potential west coast wind energy sites.

The mean wind vertical profiles are strongly influenced by local terrain inhomogeneities (6,7,8,9,10). At all stations we will therefore discuss the data from the highest sensors only. The number of observations were chosen as the maximum allowed by the computer, $N \approx 2200$ for a scalar and $N \approx 1500$ for a two-dimensional vector.

3 RESULTS

3.1 Broadbanded spectra

Figure 1 shows the estimated energy spectrum for summer at Vindenes over a broad frequency range. The low frequency part is based on hourly mean values and the higher frequency part on five minute mean values. The small difference between the two in the overlap region is random due to the two different samples. The spectral maxima near the high frequency end are not considered to be significant. They are rather interpreted to indicate Akaike's scheme to identify unnecessarily complicated AR-models for wind fluctuations (Eidsvik, 11, 12).

The Marsta (Smedman-Høgstrøm and Høgstrøm, 13) and Ås spectra in Figure 1 illustrate the high wind fluctuation level at the western coast. The spectacular Ås spectrum, with its maximum at the periods 24 hrs, 12 hrs, 6 hrs is understood as follows: The 24 hrs maximum is probably associated with the strong sea breeze most afternoons (10). The 12 hrs maximum is probably associated with the afternoon maximum and the weaker downvalley maximum wind most mornings. These maxima are absent at the west coast spectra. This is caused by weaker daily variations (more cloud cover) and/or stronger non-local contributions to the wind fluctuations.

The estimates at Vindenes are indicative of a slight spectral gap at periods of the order of minutes.

3.2 West coast spectra

The estimated west coast spectra are shown in Figures 2 a and b. At lower frequencies the spectral shape is remarkably similar at all stations both summer and winter with a power law in the neighbourhood of -2 or $-5/3$. This does also apply to the Marsta spectrum and to an envelope of the Ås spectrum. The dependence between low frequency energy and mean wind speed is remarkable (Figure 3).

Relative to the low frequency level, there seem to be significantly more small scale energy at Kårstø, Årvikafjell and Dyrholtet than at Ytraland and Vindenes. This is probably due to differences in neighbouring terrain inhomogenities.

Figures 4 and 5 indicate that the power spectra of easterly- and northerly-wind components show similar properties as the wind force. The tendency towards estimated more high-frequency energy is caused by the wind direction data being instantaneous.

3.3 Prediction error

Table 1 shows the estimates for the expected value, variance and one step ahead prediction error for the wind force and the diagonal part of \underline{Y} for the horizontal wind vector. Figure 4, which is representative for the contents of Table 1, and Figure 2, shows

the tendency for a large prediction error when the energy spectrum at the higher frequencies is high. While the low frequency energy is generally higher during the winter than summer, the prediction error varies only little with the season. This is probably due to increased (small scale) convective activity during the summer.

Roughly, the minimum prediction error for 5 min. mean wind over a lead time of 5 minutes is approximately $\sqrt{V} \approx 0.2U \approx 1 \text{ ms}^{-1}$. The 5 minutes prediction error for instantaneous wind based on instantaneous observations would be larger due to effects of small scale fluctuations. Reduction of the prediction error is obtained by choosing smaller lead times. The effectiveness of reduced lead time is determined by the stochastic properties of the smaller atmospheric eddies. For engineering purposes, it is a useful approximation to consider the smaller eddies as random walk (11, 12) implying that the prediction variance increases approximately linearly with the lead time.

4 REMARKS

The maximum model size was kept at $p = 12$ for the 5 min. data to avoid computational instabilities occurring with larger models. Since Akaike's AIC-measure may appear to identify unnecessarily complicated AR-models (11, 12), as is also indicated by the (most probably) insignificant high frequency spectral maxima, a $p \leq 12$ is considered sufficient.

The off-diagonal terms in the spectral tensor may not be negligible, but are left undiscussed because it is the wind force that is expected to be the most relevant variable for wind energy studies.

The vertical coherence of horizontal wind is expected to be close to one as long as the height separation Δz fulfils the inequality (Eidsvik, 14):

$$\Delta z \lesssim 5 \cdot 10^{-2} U / f \quad (12)$$

With a mean wind $U \approx 5 \text{ ms}^{-1}$, the vertical coherence will therefore be close to one at all frequencies considered in this study as long as $\Delta z \leq 150 \text{ m}$, a sufficient vertical distance for wind energy studies.

ACKNOWLEDGEMENTS

Anne Grete Friberg adapted Akaike's TIMESAC power spectrum program and made nonstandard data available to our computer.

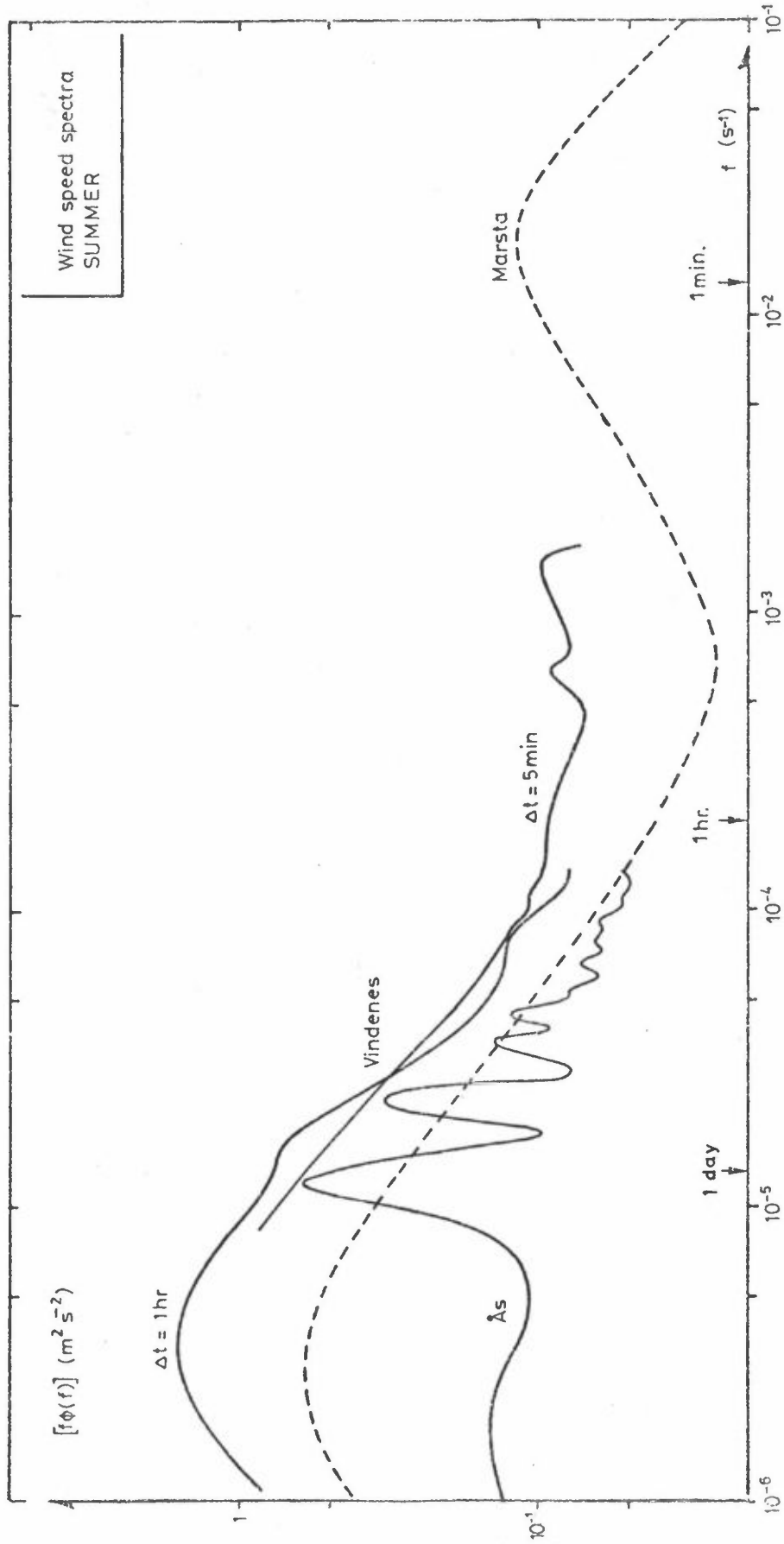


Figure 1: Estimated wind speed spectra at Vindenes (Sotra) and Ås (Telemark). The Marsta (Sweden) spectrum is obtained from Smedman-Högström and Högström (13).

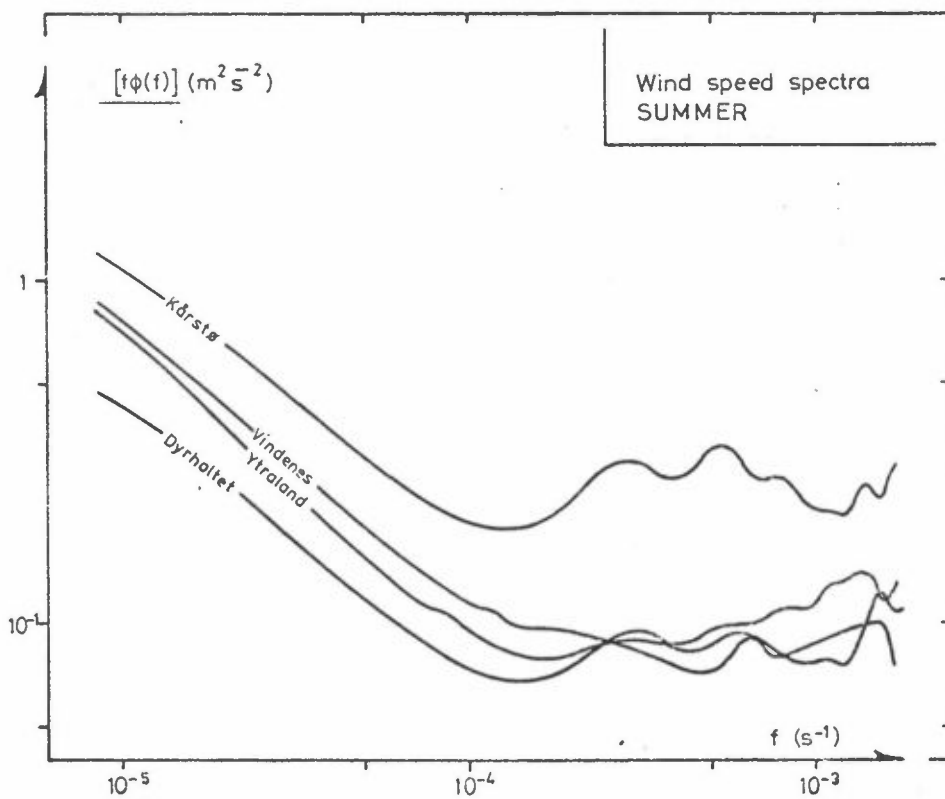


Figure 2a: Estimated wind speed spectra for the summer season.

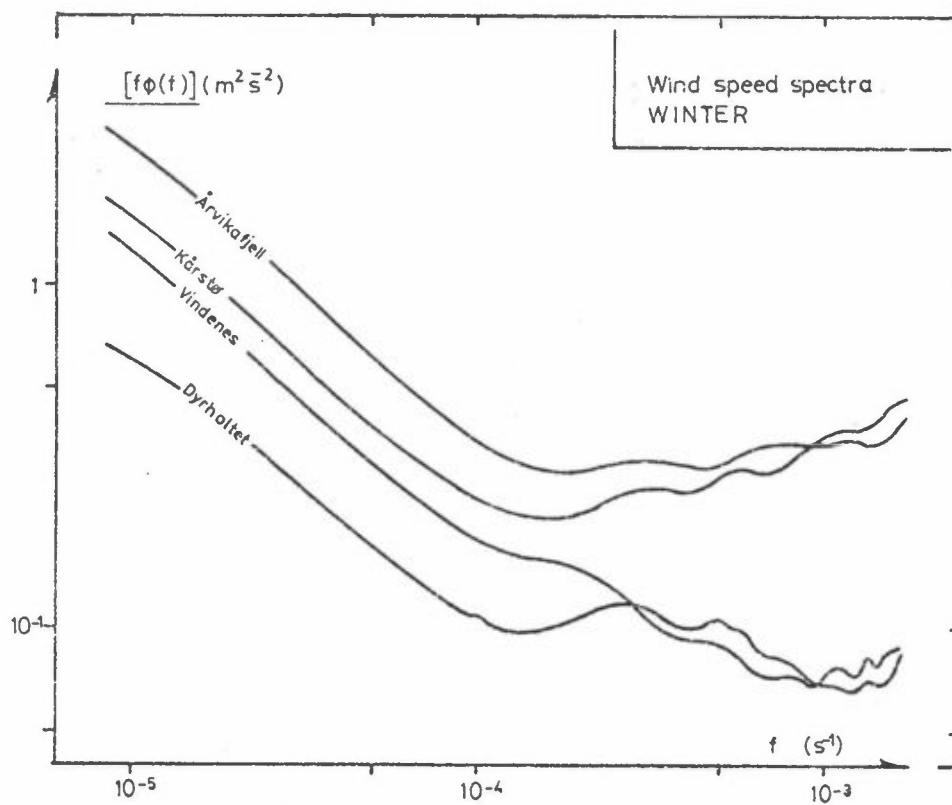


Figure 2b: Estimated wind speed spectra for the winter season.

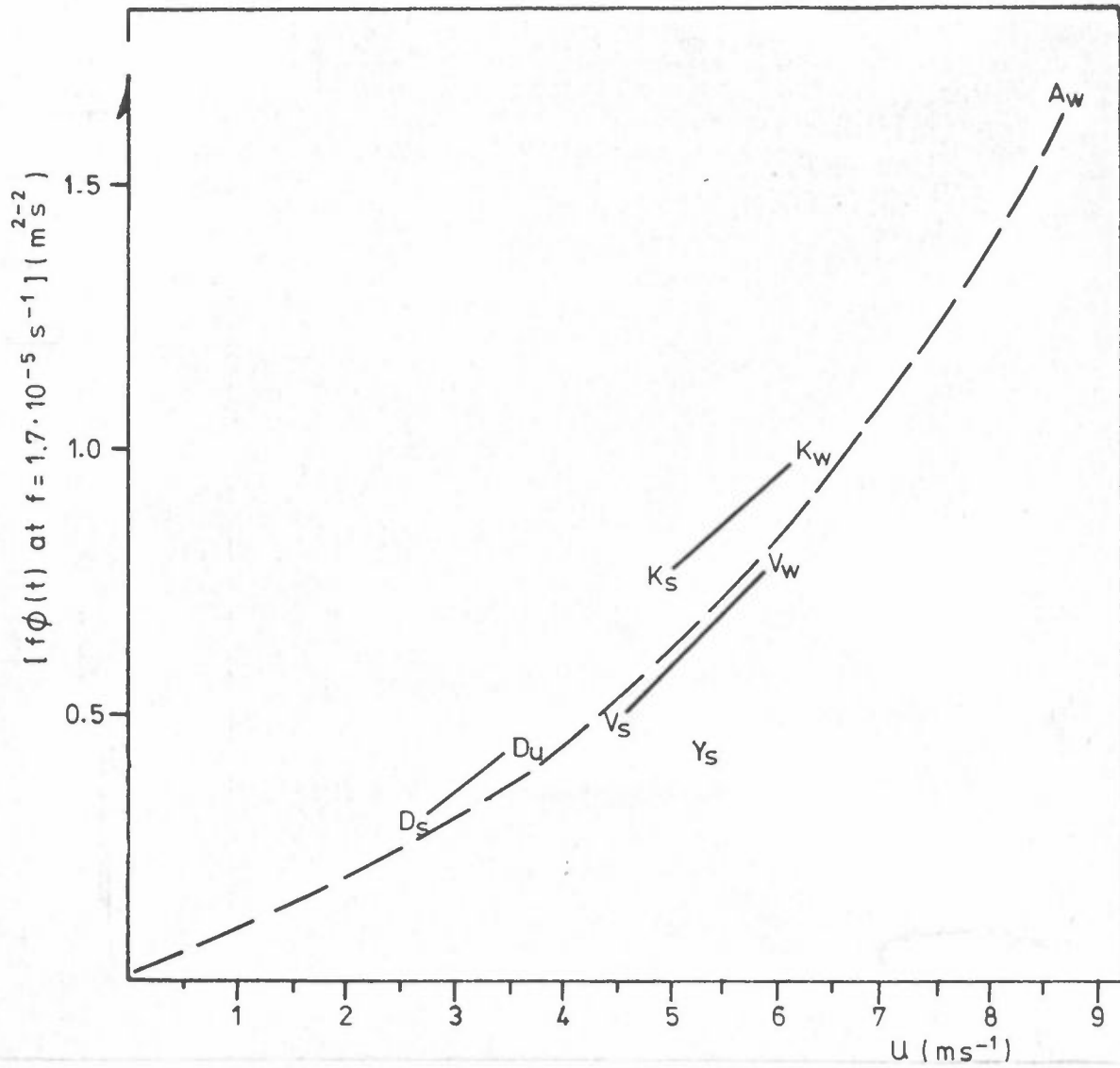


Figure 3: Spectral intensity near the daily period and mean wind speed at the different stations, summer and winter.

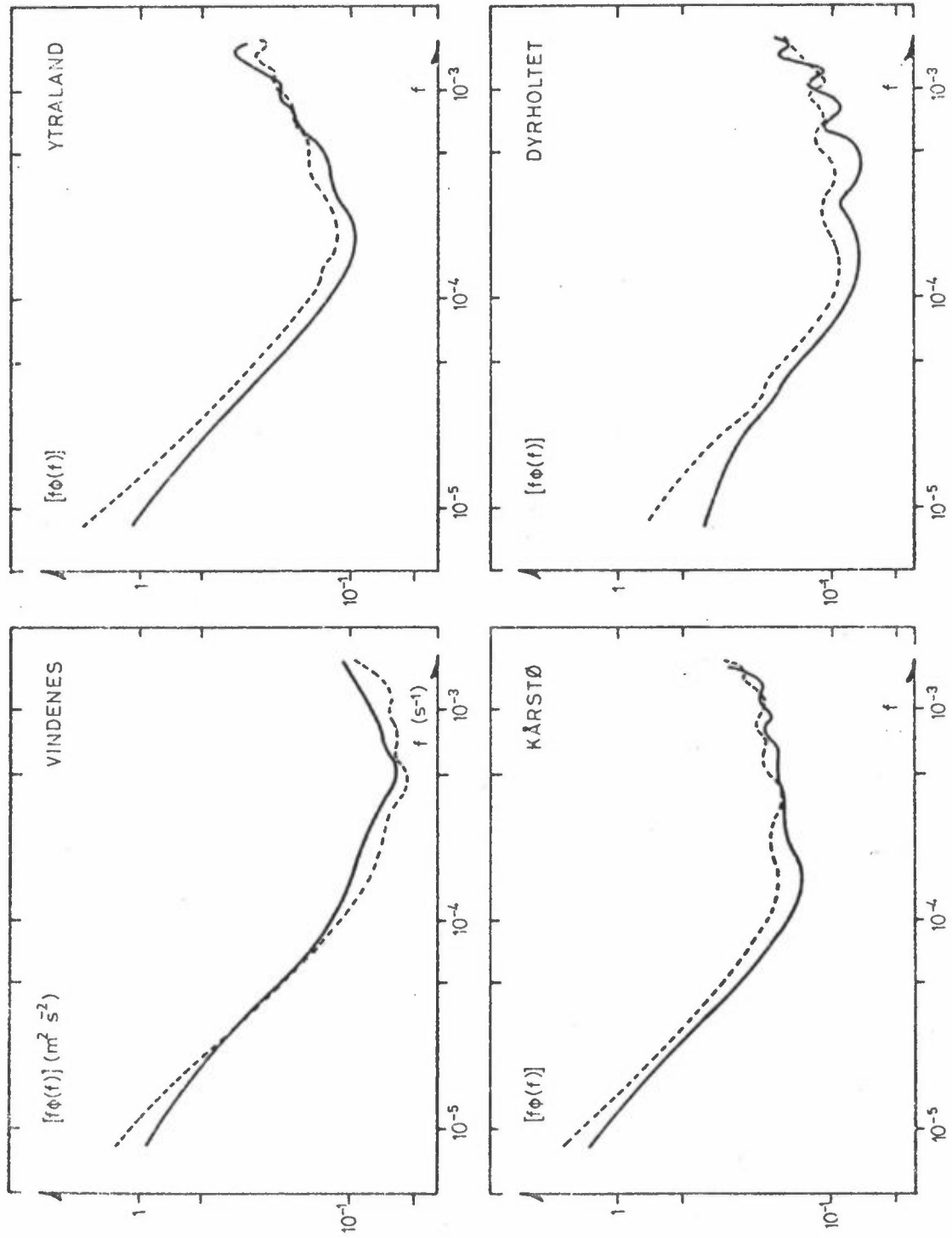


Figure 4: Estimated diagonal part of horizontal wind spectral tensor, Summer season.
——: Easterly component
-----: Northerly component

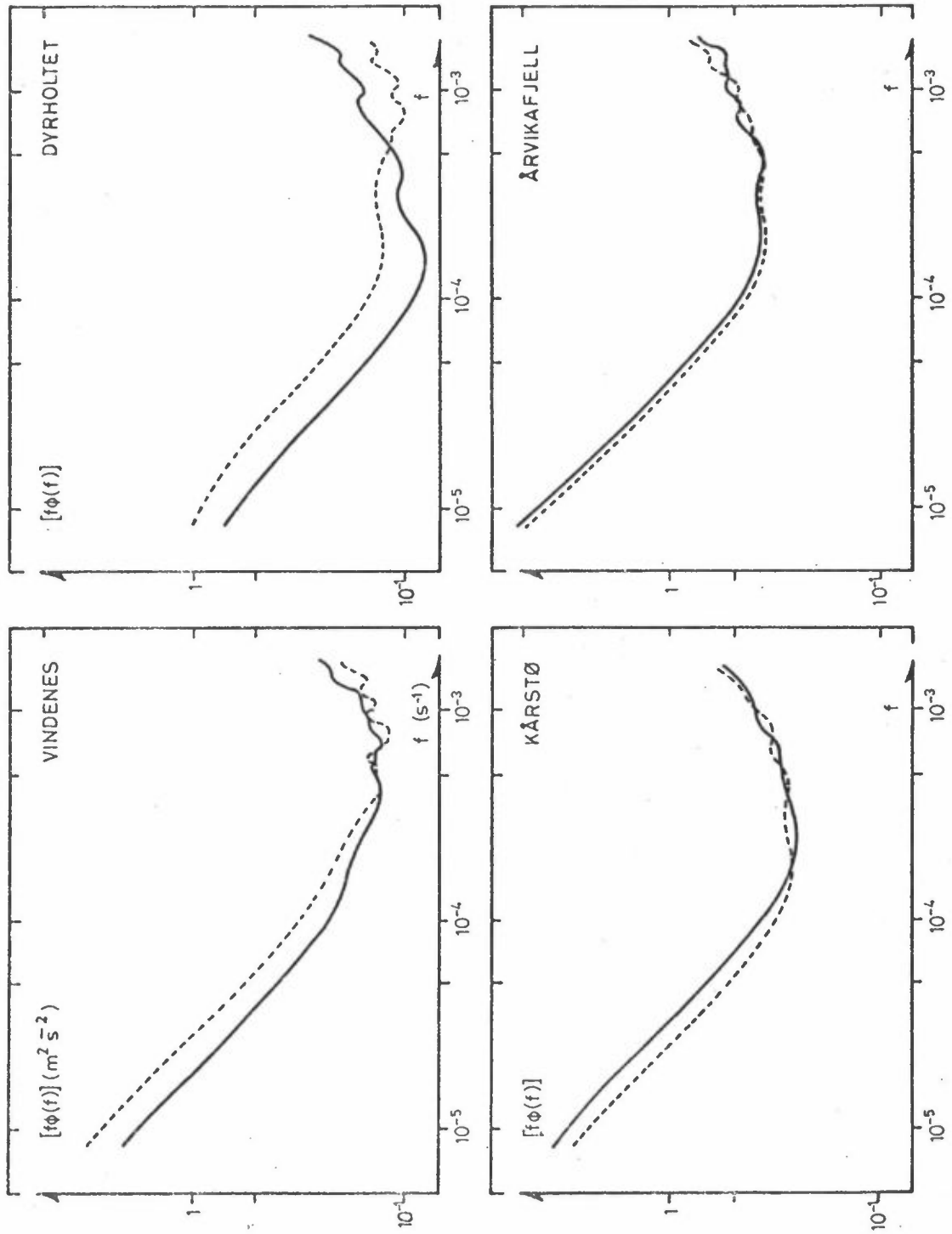


Figure 5: Estimated diagonal part of horizontal wind spectral tensor. Winter season.
——: Easterly component
-----: Northerly component

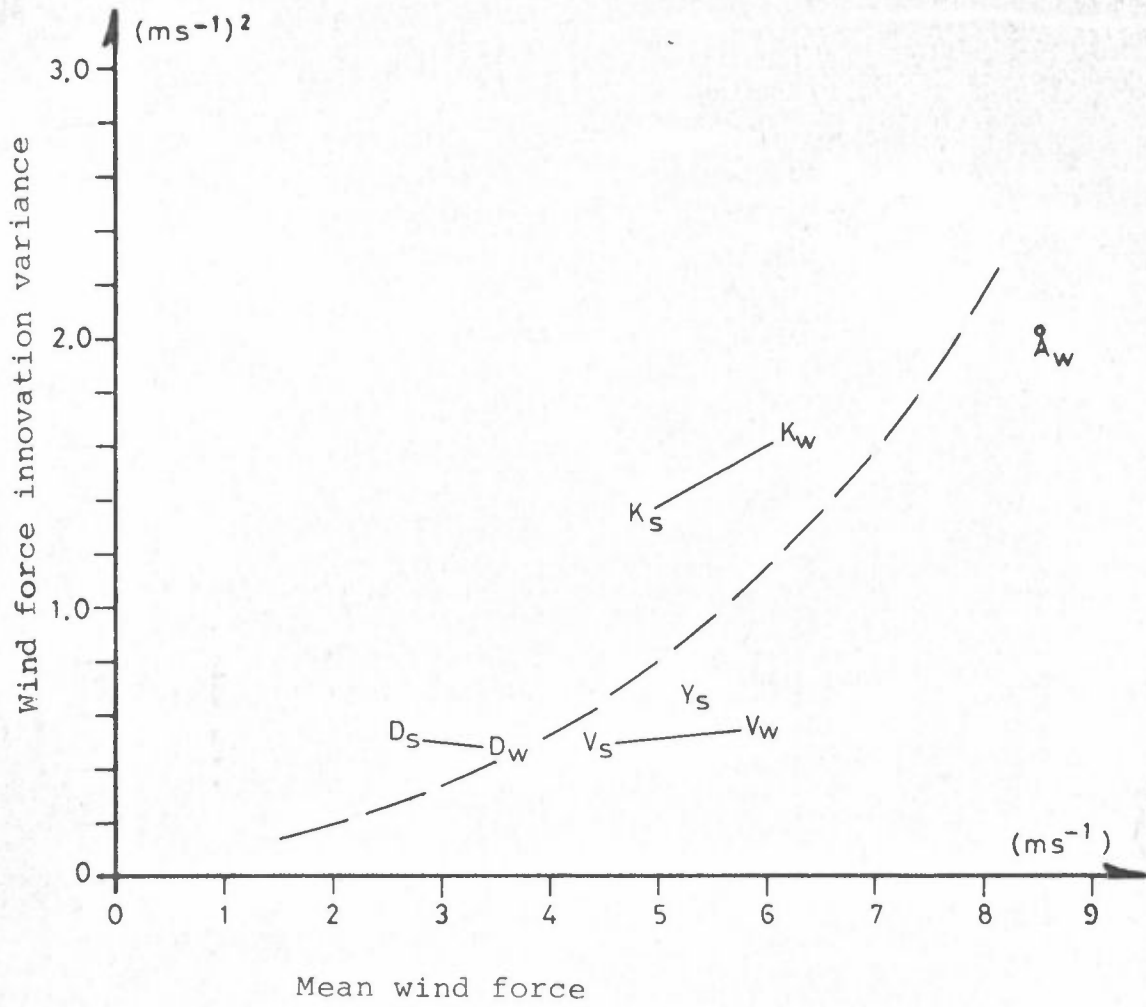


Figure 6: Estimated 5 min. wind speed prediction variance and mean wind speed at the different stations summer and winter.

Table 1: Estimates of mean value: U , climatic variance: σ^2 and innovation variance V_i for wind force: $|\underline{v}|$ and easterly and northerly wind components: (u_1, u_2) .
Summer: s and winter: w. Units: (ms^{-1}) and $(\text{ms}^{-1})^2$.

		U		σ^2		V_i	
		s	w	s	w	s	w
Vindenes	$ \underline{v} $	4.46	5.91	7.98	11.67	0.48	0.51
	u_1	0.88	0.33	6.30	20.03	0.48	0.96
	u_2	-1.15	2.74	16.73	31.14	0.41	0.93
Kårstø	$ \underline{v} $	4.87	6.2	9.46	16.33	1.36	1.81
	u_1	0.85	2.47	14.14	30.61	1.13	2.09
	u_2	-1.15	-0.78	20.56	24.18	1.21	2.11
Arvikafjell	$ \underline{v} $		8.52		24.36		1.92
	u_1		3.04		48.78		2.68
	u_2		0.44		49.77		2.71
Ytraland	$ \underline{v} $	5.24		10.60		0.62	
	u_1	0.82		10.25		1.10	
	u_2	-1.42		31.57		1.11	
Dyrholtet	$ \underline{v} $	2.6	3.5	3.67	4.95	0.50	0.47
	u_1	0.46	-1.38	3.46	6.57	0.60	0.82
	u_2	-0.23	1.55	7.07	8.33	0.67	0.72

5 REFERENCES

- (1) Athans, M., The role and use of the stochastic linear-quadratic-gaussian problem in control system design. *IEEE Trans. autom.control* AC-16, 529-552 (1971).
- (2) Parzen, E., Multiple timeseries modelling. In: *Multivariate analysis*, P.R. Krishnaiah, ed., New York, Academic Press, 1969, vol. II, pp 389-410.
- (3) Akaike, H., A new look at the statistical model identification. *IEEE Trans. autom.control*, AC-19, 716-723 (1974).
- (4) Kromer, R.E., Asymptotic properties of the autoregressive spectral estimator. Ph.D. dissertation. Stanford, Calif., 1969. (Stanford Univ. Dep. Stat., Techn. Rep. 13.)
- (5) Gersch, W.,
Sharpe, D.R. Estimation of power spectra with finite - order. Autoregressive models. *IEEE Trans. autom.control*, AC-18, 367-369 (1973).
- (6) Sivertsen, B., Meteorology, air quality and precipitation chemistry at Sotra Winter 1977/78. Lillestrøm 1978. (NILU OR 20/78).
- (7) Sivertsen, B., Meteorology, air quality and precipitation chemistry at Sotra, Summer 1978. Lillestrøm 1978. (NILU OR 53/78).
- (8) Sivertsen, B., Statfjord gas system meteorology and air quality at Kårstø. Lillestrøm 1980. (NILU OR 25/80).
- (9) Dovland, H., Vind og spredningsforhold i Mongstad-området september 1977 - august 1978. Lillestrøm 1978. (NILU OR 59/78).

- (10) Sivertsen, B.,
Friberg, A.G. Meteorologiske data fra nedre Telemark
sommeren 1979. Lillestrøm 1980.
(NILU OR 3/80).
- (11) Eidsvik, K.J., Identification of models for some
time series of atmospheric origin
with Akaike's information criterion.
J.appl.meteorol. 19 357-369 (1980).
- (12) Eidsvik, K.J., On optimal prediction of Ekman layer
fluctuations over short lead times.
In: *Proceedings of WMO Symposium on
probabilistic and statistical
methods in weather forecasting,*
Nice, 8-12 sept. 1980, pp 475-480.
- (13) Smedman-Høgstrøm, A.S., Spectral gap in surface layer
Høgstrøm, U., measurements.
J.Atmos.Sci. 32, 340-350, (1974).
- (14) Eidsvik, K.J., Measurements of mesoscale atmospheric
fluctuations in the Ekman layer
Halsemoen. Kjeller 1977. (FFI Intern
rapport VM-50.)

APPENDIX A

Spectrum estimation via ARMA-models. Summation convention on repeated indicies is used, and π -s are not accounted for.

$$A_{ij}(k)u_j(t-k) = B_{ij}(k)\epsilon_j(t-k)$$

Squaring and taking expected values gives

$$A_{ij}(k)A_{pq}^*(l)Q_{jq}(k-l) = V_{jq}B_{ij}(k)B_{pq}^*(l)\delta(k-l)$$

Here $E u_j(t-k)u_q^*(t-l) = Q_{jq}(k-l)$ and $E \epsilon_j(t-k)\epsilon_q^*(t-l) = V_{jq}\delta(k-l)$.
Introducing the power spectrum $\phi_{jk}(f)$

$$\begin{aligned} A_{ij}(k)A_{pq}^*(l)\sum_f \phi_{jk}(f)e^{2\pi if(k-l)} \\ = V_{jq}B_{ij}(k)B_{pq}^*(l)\sum_f e^{2\pi if(k-l)} \end{aligned}$$

Rearranging and summing on k and l give

$$\sum_f \{A_{ij}^F(f)A_{pq}^{F*}(f)\}\phi_{jq}(f) = \sum_f V_{jq}\{B_{ij}^F(f)B_{ij}^{F*}(f)\}$$

Here $A_{ij}^F(f)$ and $B_{ij}^F(f)$ are the Fourier transforms of $A_{ij}(k)$ and $B_{ij}(k)$. The above equation can be arranged as

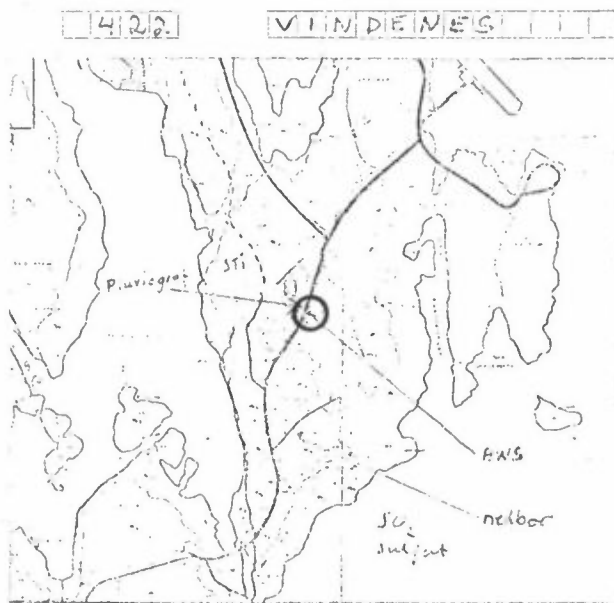
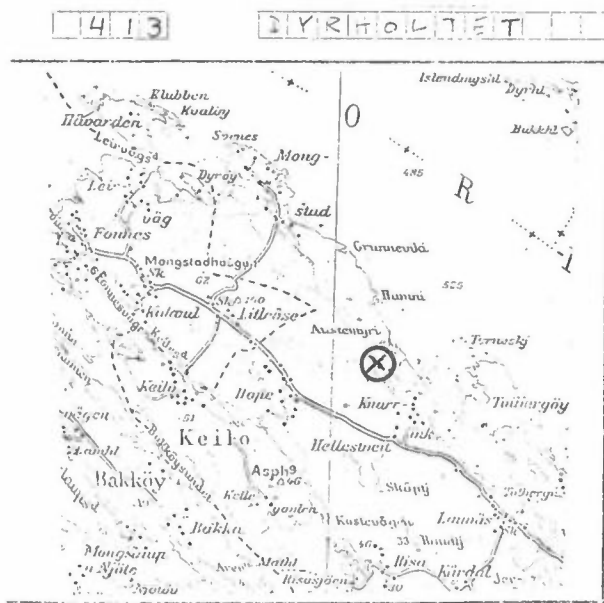
$$\sum_f [\{A_{ij}^F(f)A_{pq}^{F*}(f)\}\phi_{jq}(f) - V_{jq}\{B_{ij}^F(f)B_{pq}^{F*}(f)\}] = 0$$

Since $\phi_{jq}(f)$ and V_{jq} are positive definite, each term of the f- sum is positive. This implies that each must be equal to zero. That is:

$$\{A_{ij}^F(f)A_{pq}^{F*}(f)\}\phi_{jq}(f) = V_{jq}\{B_{ij}^F(f)B_{pq}^{F*}(f)\}$$

Q.E.D.

APPENDIX B



**N I L U**

TLF. (02) 71 41 70

NORSK INSTITUTT FOR LUFTFORSKNING(NORGES TEKNISK-NATURVITENSKAPELIGE FORSKNINGSRÅD)
POSTBOKS 130, 2001 LILLESTRØM
ELVEGT. 52.

RAPPORTTYPE Oppdragsrapport	RAPPORTNR. OR 38/80	ISBN--82-7247-206-6
DATO November 1980	ANSV. SIGN. B. Ottar <i>B. Ottar</i>	ANT. SIDER 22
TITTEL Estimering av tidsseriemodeller for horisontal vind. Vestkysten		PROSJEKTLEDER K.J. Eidsvik
		NILU PROSJEKT NR 22480
FORFATTER(E) Karl J. Eidsvik		TILGJENGELIGHET ** A
		OPPDRAUGSGIVERS REF.
OPPDRAUGSGIVER Institutt for Energiteknikk		
3 STIKKORD (å maks.20 anslag)		
Vind	Tidsseriemodell	Energi
REFERAT (maks. 300 anslag, 5-10 linjer) Tidsserier for horisontal vind med samplingsintervall $\Delta t = 5$ min er analysert. Energispektra er estimert via tilpasning av autoregressive modeller. Akaike's identifikasjonsmetode er anvendt.		
TITLE Estimation of timeserie models for horizontal wind. Norwegian west coast.		
ABSTRACT (max. 300 characters, 5-10 lines) Timeseries of horizontal wind sampled at intervals of $\Delta t = 5$ min are analyzed. Power spectra are estimated via autoregressive model fitting. Akaike's identification procedure is used.		

**Kategorier: Åpen - kan bestilles fra NILU A
Må bestilles gjennom oppdragsgiver B
Kan ikke utleveres C